Demixing and Remixing Kinetics in Aqueous Dispersions of Poly(N-isopropylacrylamide) (PNIPAM) Brushes Bound to Gold Nanoparticles Studied by Means of Modulated Temperature Differen...

5 AUTHORS, INCLUDING:

Jun Zhao
National Center for Nanoscience and Techn…
84 PUBLICATIONS **828** CITATIONS

SEE PROFILE

Guy Van Assche
Vrije Universiteit Brussel
129 PUBLICATIONS **1,791** CITATIONS

SEE PROFILE

Heikki Tenhu
University of Helsinki
215 PUBLICATIONS **5,334** CITATIONS

SEE PROFILE

Macromolecules

ARTICLE

Demixing and Remixing Kinetics in Aqueous Dispersions of Poly(N-isopropylacrylamide) (PNIPAM) Brushes Bound to Gold Nanoparticles Studied by Means of Modulated Temperature Differential Scanning Calorimetry

Jun Zhao,[†] **Jun Shan,**[‡] **Guy Van Assche,**[†] **Heikki Tenhu,**[‡] **and Bruno Van Mele*,**[†]

[†]*Department of Physical Chemistry and Polymer Science, Faculty of Engineering Sciences, Vrije Universiteit Brussel, Pleinlaan 2, 1050 Brussels, Belgium, and* [‡]*Laboratory of Polymer Chemistry, Department of Chemistry, University of Helsinki, PB 55, FIN-00014 HY, Finland*

Received April 3, 2009; Revised Manuscript Received June 1, 2009

ABSTRACT: The demixing and remixing kinetics in aqueous dispersions of poly(N-isopropylacrylamide) (PNIPAM) brushes covalently bound to the surface of the gold nanoparticles, which are denoted as Au−PNIPAM, is studied by means of modulated temperature differential scanning calorimetry (MTDSC) in both nonisothermal and quasi-isothermal modes. The nonisothermal measurements show double demixing peaks in both the heat flow and the heat capacity traces for dispersions with a weight fraction of Au−PNIPAM (f_w) below 50 wt %. The lower phase transition corresponds to an inner layer of PNIPAM segments on the surface of the gold core, while the upper transition corresponds to an outer layer. The dispersions follow a lower critical solution temperature phase behavior with a threshold demixing temperature at about 11.4 °C for f_w of 45.3 wt %. Comparison with aqueous solutions of PNIPAM with different molar masses shows that the gold core reduces the miscibility of PNIPAM with water. The process kinetics throughout the phase transition is studied by quasi-isothermal heat capacity measurements, through the effect of the modulation frequency, by changing the heating rate and repeated heating−cooling cycles. Overall, the response for Au−PNIPAM dispersions is markedly faster than for PNIPAM solutions, which might be the result of water remaining finely dispersed within the polymer matrix. Close to the gold core, the restricted collapse of the PNIPAM chains, as a result of steric hindrance by neighboring anchored chains, might result in the presence of water inside the collapsed nanoparticle. Notwithstanding the occurrence of partial vitrification in the polymer-rich phase during heating, the Au−PNIPAM dispersions retain their thermoresponsive behavior after repeated heating−cooling cycles.

Introduction

Aqueous solutions of water-soluble polymers such as poly(N-isopropylacrylamide) (PNIPAM),[1–18] poly(2-isopropyl-2-oxazoline) (PIPOZ),[19–23] poly(N-vinylcaprolactam) (PVCL),[24–30] and poly(methyl vinyl ether) (PMVE)[15,31–38] exhibit demixing at physiological temperatures, which can be interesting toward applications like controlled drug release and thermoresponsive membranes.[5,31] Their phase separation follows the lower critical solution temperature (LCST) phase behavior, which means that the solutions are in a homogeneous state at low temperature while they demix during heating and are in a heterogeneous state at high temperature. According to a proposed classification,[39] aqueous solutions of PNIPAM follow type II LCST demixing behavior,[40] which is also confirmed in our previous work using modulated temperature differential scanning calorimetry (MTDSC).[11]

MTDSC is a powerful extension of conventional differential scanning calorimetry (DSC), in which a sinusoidal perturbation is superimposed on the underlying temperature program. MTDSC allows for the simultaneous measurement of heat flow, heat capacity, and heat flow phase. In the study of polymer materials by means of MTDSC, the kinetic thermal processes, depending on time and absolute temperature, usually appear in the nonreversing heat flow (HF_{nonrev}), while properties with heat effects proportional to the heating rate are found in the reversing heat flow (HF_{rev}) or heat capacity (c_p) related signal. In this case, the HF_{rev} signal equals the average heating rate times the measured specific heat capacity (c_p), which is calculated as

$$c_p = \frac{A_{HF}}{A_T \omega} \tag{1}$$

where $A_T \omega$ is the amplitude of the imposed modulated heating rate, with A_T the temperature modulation amplitude, ω the modulation angular frequency ($= 2\pi/p$), and p the modulation period; A_{HF} is the amplitude (of the first harmonic) of the resulting modulated heat flow. HF_{nonrev} equals the total heat flow (HF_{tot}) (the running average of the modulated signal) minus HF_{rev}. A complete description of the extraction of the heat capacity and other MTDSC signals can be found in the literature.[41–44]

This straightforward MTDSC deconvolution of c_p and thermal transformations in separate signals turns out to be very valuable for the study of the kinetics and chemorheology in reacting systems.[45–47] However, it is no longer valid for the characterization of fast processes, e.g., melting/crystallization,[48–52] temperature-induced phase separation in blends[53–55] and solutions,[11,14,15,18,26,35,37,38] and reaction-induced phase separation in reacting systems.[55,56] Heat effects caused by these fast processes can occur during each modulation cycle and thus contribute to A_{HF} in eq 1 and to the c_p signal derived from it. Hence, the c_p

*To whom correspondence should be addressed: Tel + 32-2-6293276, Fax + 32-2-6293278, e-mail bvmele@vub.ac.be.

signal calculated by eq 1 contains a so-called excess contribution (c_p^{excess}) in addition to the baseline specific heat capacity (c_p^{base}) and is therefore called the apparent (specific) heat capacity.

$$c_p^{app}(T, t) = c_p^{base}(T) + c_p^{excess}(T, t) \qquad (2)$$

c_p^{base} is based on thermodynamics and is (to a good approximation) only temperature-dependent. c_p^{excess} originates from the fast processes at the interface of coexisting phases and changes with the progress of the phase transformation, e.g., morphology development. As c_p^{excess} is temperature- and time-dependent, c_p^{app} is also temperature- and time-dependent and changes during the phase transformation.

MTDSC can be used to study the phase separation in both nonisothermal and quasi-isothermal (average heating rate equal to zero) conditions. For the nonisothermal measurements, during phase separation, the fast demixing/remixing processes following the applied temperature modulation will give rise to a c_p^{excess} superimposed on c_p^{base}. This feature enables the complete construction of the state diagram by means of nonisothermal c_p^{app} measurements.[11,14,15,18,26,35,37,38,53-55] For the quasi-isothermal measurements, the time-dependent behavior of c_p^{app} (and c_p^{excess}) in the phase separation region can provide additional information on the fast molecular processes of demixing and remixing (nanoscale miscibility) at the interface of coexisting phases and on the long-term evolutions (slow processes) of this interface fraction toward an equilibrium condition (morphology development on a macroscopic level), which is independent of the thermal history and the phase separation kinetics.[11,14,18,26,35,38,53-55] Thus, the quasi-isothermal measurements make the real-time monitoring of the temperature- or reaction-induced demixing and remixing possible.[55]

In our previous study of the demixing and remixing kinetics in aqueous solutions of PNIPAM, it is found that in the transition region c_p^{app} (and c_p^{excess}) during cooling is lower than during heating, which indicates that remixing is a slower process than demixing.[11] This effect is accentuated by the partial vitrification of the PNIPAM-rich phase, which is usually not taken into account for aqueous solutions of polymers. However, a high degree of partial vitrification can increase the remixing time significantly.

Aqueous solutions of polymer brushes show a different phase behavior from solutions of free polymer chains because for the polymer brushes grafted on a substrate, strong interchain interactions are present in the zone close to the surface of the substrate, which is distinct from free chains in solutions adopting a random coil conformation.[57] Surface plasmon resonance spectroscopy has shown that PNIPAM brushes grafted from a mixed self-assembled monolayer on a bulk gold surface undergo a quite broad transition with no sharp changes over a range of temperatures.[8] In contrast, contact angle measurements which are sensitive to the outermost 5−10 Å of the surface reveal a sharp change.[8] For tethered PNIPAM layers grafted on polystyrene latex particles, the aqueous dispersions show a phase transition in a wider temperature range than in the case of the coil−globule transition of free PNIPAM chains in aqueous solutions.[58] Dilute aqueous dispersions of PNIPAM brushes covalently bound to the surface of gold nanoparticles (denoted as Au−PNIPAM) have been reported to exhibit two separate phase transitions.[59] The double demixing peaks in high-sensitivity microcalorimetry are explained by a model of double subzones.[59] That is to say, the PNIPAM brushes can be subdivided into two zones: an inner layer and an outer layer. In the inner layer, the PNIPAM segments are close to the gold surface, densely packed, less hydrated, and undergo the lower (temperature) transition. In the outer layer, on the other hand, the PNIPAM segments are looser and more hydrated and undergo the upper (temperature)

transition. Very recently, the effect of molar mass and gold core size on the phase transition of Au−PNIPAM oligomers has been reported.[60] For these samples, there is only the inner layer due to the low molar mass, and therefore only the lower (temperature) transition exists. It is found that both decreasing molar mass and increasing gold core size cause lower phase transition temperature. Recently, double phase transitions of PNIPAM grafted on a hydrophobic hyperbranched polyester core have also been reported.[61,62]

In this work, the above-mentioned MTDSC concepts for aqueous solutions will be used to investigate the demixing and remixing kinetics in aqueous dispersions of Au−PNIPAM over the full range of concentrations. A comparison to the aqueous solutions of pure PNIPAM will be made to study the effect of the gold core. The different properties of the double phase transitions will be discussed in terms of the concept of double subzones.[59]

Experimental Section

Materials. Cumyl-PNIPAM-gold nanoparticles with PNIPAM chains (M_n = 4700 g mol⁻¹, M_w/M_n = 1.1) grafted to a gold core were synthesized and purified as described elsewhere.[59,63] They are denoted here as Au−PNIPAM. The average number of gold atoms for each core is about 79. The average number of PNIPAM chains for each gold core is about 30, leading to a high grafting density.[59,63] Pure PNIPAM (M_n = 24 700 g mol⁻¹, M_w/M_n = 3.0), denoted as PNIPAM-25K, was obtained from Polysciences Inc. Water was deionized with a Millipore Milli-Q water purification system.

Dispersions Preparation. Dispersion concentrations are expressed as weight fractions of Au−PNIPAM (f_w). As the gold core amounts to about 10.0 wt % of the total mass of a Au−PNIPAM particle, the weight fraction of PNIPAM in the dispersion is about a factor 1.11 lower.[59,63] Starting from a dilute dispersion of Au−PNIPAM in water with f_w of about 1.1 wt %, a full range of compositions was prepared directly in TA Instruments T_{zero} hermetic aluminum crucibles of 40 μL. More concentrated dispersions were prepared by drying the initial dispersion in air at ambient temperature to the target f_w. The final dispersions for the subsequent MTDSC measurements had a mass of about 2.5 mg. All the hermetically sealed crucibles were put in the refrigerator horizontally with the lid side upward and kept at 4 °C for at least 24 h to obtain a homogeneous state. A few of the closed crucibles were perforated and the weight loss was measured at 100 °C using thermogravimetric analysis (TA Instruments Q5000 TGA) to check the preparation procedure (relative error of f_w < 1.0%). For comparison, an aqueous solution of PNIPAM-25K with f_w of 50.0 wt % was prepared accordingly.

MTDSC Measurements. The first series of MTDSC measurements were performed on a TA Instruments Q2000 DSC (T_{zero} DSC technique) with the MDSC option, equipped with an RCS cooling accessory and purged with nitrogen (50 mL min⁻¹). The second series of MTDSC measurements were performed on a TA Instruments TA2920 DSC with the MDSC option, equipped with an RCS cooling accessory and purged with helium (50 mL min⁻¹). Baseline, heat capacity, and temperature were calibrated with sapphire (for Q2000 DSC), poly(methyl methacrylate) (for TA2920 DSC), and indium (for both). The hermetic crucibles were perforated for the measurements of pure Au−PNIPAM. The standard modulation conditions with A_T of 0.5 K and p of 60 s were used unless stated otherwise. Scan rates were 1.0 and 2.5 K min⁻¹ for phase separation measurements and glass transition measurements, respectively, unless stated otherwise. For phase separation measurements, the dispersions were kept isothermally for 30 min at a lower limit temperature of 2.0 °C or −10.0 °C (depending on f_w of the dispersions) and for 5 min at an upper limit temperature of 65.0 °C. For glass transition measurements, the dispersions were kept isothermally for 10 min at a lower limit temperature of −60.0 °C and for 1 min
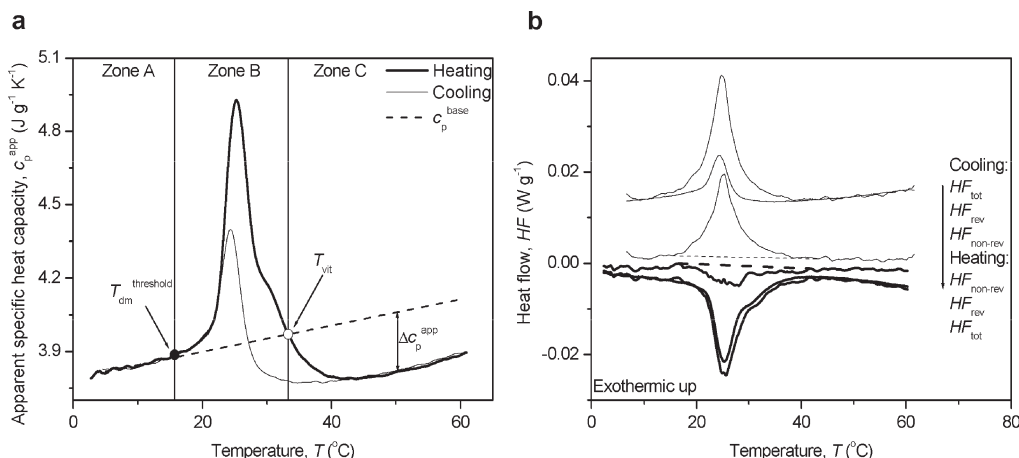
Figure 1. MTDSC c_p^{app} (a) and HF (b) traces for the nonisothermal demixing (heating, thick curves) and subsequent remixing (cooling, thin curves) of an aqueous Au−PNIPAM dispersion with f_w of 21.1 wt %. In (a), $T_{dm}^{threshold}$ by 0.01 J g^{-1} K^{-1}, T_{vit}, and Δc_p^{app} (at 50.0 °C) are shown. In (b), HF_{tot}, HF_{rev}, and HF_{nonrev} are given. All HF curves in (b) are shifted vertically for clarity. Dashed lines in (b) represent baselines for HF_{nonrev}.

at an upper limit temperature of 65.0 °C (or 180.0 °C for pure Au−PNIPAM). Three heating−cooling cycles were run to control the reproducibility. For most measurements, all three cooling runs coincide very well. Only the first heating run was slightly different from the subsequent two heating runs, which might be due to sample preparation effects. To reduce these effects, the second cycle was used for the analysis of demixing and remixing, while the second cooling and the third heating were used for the analysis of glass transition.

Cloud Point Measurements. The cloud points of Au−PNI-PAM dispersions were determined by measuring the light transmitted by thin samples between glass slides mounted in a Mettler-Toledo FP82HT hot stage, which was placed in a Spectratech optical microscope (at 10× magnification) equipped with a photodetector (most sensitive at a wavelength of 615 nm). The evaporation of water was avoided by using a 100 μm spacer adhering to the glass slides. Temperature calibration was performed with benzophenone (melting temperature is 48.1 °C) supplied by Fluka. All samples were heated from 0.0 to 50.0 °C at 1.0 K min^{-1}; a (cold) nitrogen gas purge was used for cooling below room temperature. The temperature at a 1.0% in the decrease of the light transmittance (against 100% for the transparent homogeneous dispersion) during heating was chosen as the cloud point.

Results and Discussion

Au−PNIPAM/Water State Diagram. (MT)DSC was used to study the nonisothermal demixing and remixing in aqueous dispersions of Au−PNIPAM with weight fractions f_w from 1.1 to 83.5 wt %. Figure 1a,b shows MTDSC results for the nonisothermal demixing (heating) and subsequent remixing (cooling) of an aqueous Au−PNIPAM dispersion with f_w of 21.1 wt %. Parts a and b of Figure 1 show the evolution of c_p^{app} and the heat flows, respectively, for both heating and cooling.

As for the aqueous PNIPAM solutions,[11] the demixing during heating is observed as a peak in c_p^{app} (Figure 1a), indicating a c_p^{excess} contribution arising from fast demixing/remixing processes following the applied temperature modulation. As before,[11] the demixing temperature was defined as the temperature at which the c_p^{app} increases 0.01 J g^{-1} K^{-1} above the extrapolated baseline heat capacity (denoted as $T_{dm}^{threshold}$). Most commonly, a single demixing peak is observed for aqueous solutions of water-soluble polymers.[1−3,6,7,9,11,20,26,35,64] However, double phase transitions were reported in the dilute aqueous dispersions of Au−PNIPAM (0.0025−0.02 wt %) and explained by the concept

of double subzones.[59] Although the two demixing peaks observed in Figure 1a are less well separated for the much more concentrated aqueous Au−PNIPAM dispersion with f_w of 21.1 wt %, double demixing peaks can still be distinguished in c_p^{app}.

It is well-known that aqueous PNIPAM dispersions have lower c_p values at temperatures just above the demixing region than just below this region.[2,3,6,64] For aqueous PNIPAM solutions, this c_p (or c_p^{app}) gap could be primarily attributed to a partial vitrification of the polymer-rich phase formed during demixing.[11] It is a result of the intersection of the LCST curve with the glass transition−composition curve. Figure 1a shows that this c_p gap (Δc_p^{app}) also exists for the aqueous Au−PNIPAM dispersion with f_w of 21.1 wt %. The temperature at which c_p^{app} starts to be lower than the extrapolated c_p^{base} or, in other words, the temperature at which the c_p^{base} extrapolated from the homogeneous state intersects with the c_p^{app} trace is denoted as T_{vit}. Using $T_{dm}^{threshold}$ and T_{vit}, three temperature regions can be defined: zone A, homogeneous; zone B, heterogeneous without interference of vitrification; and zone C, heterogeneous with partial vitrification of a polymer-rich phase.[11]

As shown in Figure 1a, for the aqueous Au−PNIPAM dispersion with f_w of 21.1 wt %, the area underneath the c_p^{app} curve during cooling (the remixing enthalpy) is much smaller than during the previous heating (the demixing enthalpy), which indicates that the remixing process is a slower process than the demixing, in accordance with our results on PNIPAM.[11] For temperatures outside the phase transition region, both c_p^{app} curves coincide.

In Figure 1b, the heat flow signals of the same MTDSC measurement are shown. The HF_{tot} signal corresponds to what would be observed in a conventional DSC measurement at the same heating rate. In heating, it shows an endothermic demixing (hydrogen bond disruption between polymer segments and water molecules) starting near 20 °C and ending near 40 °C. In cooling, an exothermic remixing (hydrogen bond formation between polymer segments and water molecules) occurs in the same temperature interval. It is worth noting that the remixing enthalpy obtained from HF_{tot}, written as ΔH_{rm}^{tot}, is the same (with opposite sign) as the demixing enthalpy ΔH_{dm}^{tot} during the previous heating, within the uncertainty limits of ΔH, indicating that the demixing can be reversed on the time scale of the cooling run. In addition to HF_{tot}, its separation into the heat capacity based HF_{rev} and HF_{nonrev} is given in Figure 1b.

As a result of the different evolution of c_p^{app} (and thus of HF_{rev}) for heating and cooling, the separation of HF_{tot} into HF_{rev} and HF_{nonrev} also differs. During heating, almost the entire endothermic demixing peak can be seen in HF_{rev}; only a shallow peak is left in HF_{nonrev}. During the subsequent cooling, the exothermic remixing peak is distributed over both HF_{rev} and HF_{nonrev}. As HF_{rev} and c_p^{app} contain less noise than HF_{tot} and HF_{nonrev}, and as c_p^{app} can also be followed in quasi-isothermal conditions, both advantages of MTDSC
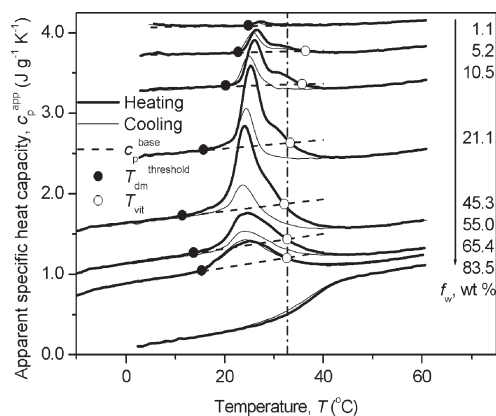

Figure 2. MTDSC c_p^{app} traces during nonisothermal demixing (heating, thick curves) and subsequent remixing (cooling, thin curves) in aqueous dispersions of Au−PNIPAM. f_w is indicated. $T_{dm}^{threshold}$ by 0.01 J g^{-1} K^{-1}, c_p^{base}, and T_{vit} are shown. All curves are shifted vertically for clarity, using the same shift for the heating and cooling curves of the same f_w.

over standard DSC,[41−44] the c_p^{app} signal will be primordially used for the discussion in this paper.

Figure 2 shows MTDSC c_p^{app} traces during the nonisothermal demixing (heating) and subsequent remixing (cooling) of aqueous Au−PNIPAM dispersions with compositions f_w ranging from 1.1 to 83.5 wt %. Double demixing peaks can be seen for dispersions with f_w below 50 wt %. For more concentrated dispersions, there is only a single demixing peak. When f_w is increased to 83.5 wt %, no demixing peak can be seen; however, a glass transition is observed around 35.8 °C. With increasing f_w, $T_{dm}^{threshold}$ first decreases, reaching a minimum, and subsequently increases again.

The decrease of c_p^{app} below c_p^{base}, as described for Figure 1a, is seen in Figure 2 for all dispersions in which demixing occurs. For dispersions with f_w of 21.1 wt % or above, the average T_{vit} is 32.7 ± 0.3 °C. A slightly higher T_{vit} is found for the dispersions of 5.2 and 10.5 wt %. It should be noted that this temperature is somewhat influenced by the process kinetics and experimental conditions[11] and the extrapolation of the c_p^{base}, which results in a larger uncertainty for smaller demixing peaks.

Figure 2 also shows that the c_p^{app} curve during cooling is lower than during the previous heating for all dispersions except the one with f_w of 65.4 wt %. For temperatures outside the phase transition region, both c_p^{app} curves coincide in all cases. It is worth noting that for f_w of 10.5 wt % and lower a double remixing peak is observed.

Figure 3a summarizes the characteristic temperatures of the nonisothermal demixing shown in Figure 2: $T_{dm}^{threshold}$ (threshold temperature of the demixing peak by 0.01 J g^{-1} K^{-1}),
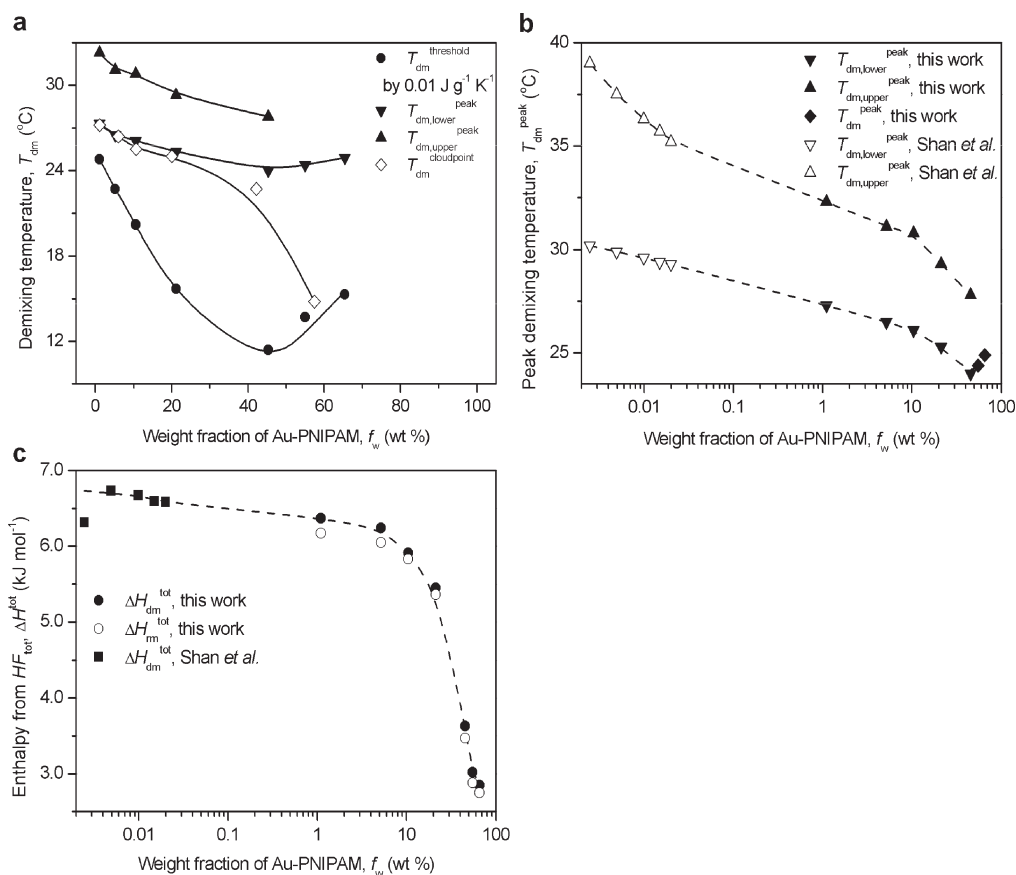

Figure 3. Effect of f_w on the demixing temperature (a, b) and demixing enthalpy (c) obtained using MTDSC for aqueous dispersions of Au−PNIPAM and their comparison with microcalorimetry data for dilute aqueous dispersions of Au−PNIPAM (from ref 59). In (a), $T_{dm}^{threshold}$, $T_{dm,lower}^{peak}$, $T_{dm,upper}^{peak}$, and $T_{dm}^{cloud\ point}$ are given. In (b), $T_{dm,lower}^{peak}$ and $T_{dm,upper}^{peak}$ are compared to values from ref 59. In (c), ΔH_{dm}^{tot} and ΔH_{rm}^{tot} are given and compared to ΔH values from ref 59. ΔH is based per mole of PNIPAM repeat units. Note the logarithmic coordinate of f_w in (b) and (c).

$T_{dm,lower}^{peak}$ (peak temperature of lower temperature demixing peak), and $T_{dm,upper}^{peak}$ (peak temperature of upper temperature demixing peak). $T_{dm}^{threshold}$ shows that the dispersions follow an LCST phase behavior with a minimum at 11.4 °C for a 45.3 wt % dispersion. A similar but less pronounced behavior is observed for $T_{dm,lower}^{peak}$. For comparison, the cloud point detected by light transmittance $T_{dm}^{cloud\ point}$ is also shown. For dispersions with f_w between 1 and 20 wt %, $T_{dm}^{cloud\ point}$ is just below $T_{dm,lower}^{peak}$ and well above the start of the demixing $T_{dm}^{threshold}$. This indicates well that the cloud point cannot be used as a marker for the onset of the demixing process of the PNIPAM brushes on the gold nanoparticles. In this case, the cloud point cannot be used to rationalize the threshold deviation of the extrapolated baseline heat capacity used for determining $T_{dm}^{threshold}$, as was done for aqueous solutions of PNIPAM,[11,65] PVCL,[26] and PMVE.[35] Hence, the 0.01 J g^{-1} K^{-1} threshold used for PNIPAM solutions[11,65] was also used in this work. Interestingly, for higher concentrations, the difference between $T_{dm,lower}^{peak}$ and $T_{dm}^{cloud\ point}$ increases, with $T_{dm}^{cloud\ point}$ moving abruptly closer to $T_{dm}^{threshold}$ for f_w of 57.4 wt % (see further discussion below).

$T_{dm,lower}^{peak}$ and $T_{dm,upper}^{peak}$ obtained by MTDSC in this work for f_w ranging from 1.1 to 83.5 wt % can be compared to results for (very) dilute solutions with f_w ranging from 0.0025 to 0.02 wt % obtained in previous work[59] by high-sensitivity microcalorimetry (Figure 3b). A smooth connection (dashed lines) between the two data sets is observed, which indicates the consistence of the two characterization methods. Good consistence is also found for the demixing enthalpies (Figure 3c). For dilute dispersions, the demixing enthalpy levels off at about 6.5−6.7 kJ per mole of PNIPAM repeat units, which corresponds approximately to the energy required to break one hydrogen bond per polymer repeat unit.[9,64,66] For comparison, the linear PNIPAM with high molar mass has a value of ΔH_{dm}^{tot} of 5.5−7.5 kJ mol^{-1}.[2,3,6,7,9,64,66] The decrease of ΔH_{dm}^{tot}, especially for f_w above 20 wt %, is due to the decreasing hydration of the polymer chains. As a result of steric hindrance in more concentrated dispersions, more repeat units cannot get access to water molecules. Thus, a lower fraction of repeat units forms hydrogen bonds with water molecules during the cooling (remixing), and the number of hydrogen bonds per repeat unit broken in the subsequent heating (demixing) is also smaller. For the whole range of f_w, ΔH_{dm}^{tot} is just slightly lower than ΔH_{rm}^{tot}. This means that almost all the hydrogen bonds broken during the heating (demixing) can be formed during the following cooling (remixing).

Figure 4 shows the comparison between $T_{dm}^{threshold}$ in aqueous Au−PNIPAM dispersions and in aqueous solutions of PNIPAM with different chain lengths (data from ref 11 for the same threshold value of 0.01 J g^{-1} K^{-1}). The aqueous solutions of PNIPAM follow the type II LCST phase behavior with the minimum independent of the chain length.[39,40] The aqueous dispersions of Au−PNIPAM have a similar behavior, however, with a minimum about 12.5 K lower. Clearly, the presence of the gold core reduces the miscibility of PNIPAM with water, which is probably due to the gold core's confining effect on the segments close to it. It is worth noting that the more sharply increasing lower concentration side of the LCST curve for Au−PNIPAM can be attributed to the lower molar mass (4700 g mol^{-1}) of the PNIPAM chains in Au−PNIPAM, as corroborated by the PNIPAM results.

Figure 5 shows MTDSC c_p^{app} traces for the cooling of concentrated aqueous Au−PNIPAM dispersions and pure Au−PNIPAM. For the pure Au−PNIPAM, a well-defined glass transition with the middle point temperature (T_g) of about 136.1 °C is observed. As expected, T_g rapidly decreases

with the addition of water: for a dispersion with f_w of 83.5 wt %, T_g drops to about 35.8 °C. When f_w is further decreased to 65.4 wt %, a glass transition at about −35.8 °C can still be seen after remixing about 40 K higher. For f_w below 65.4 wt %, the crystallization of water cannot be avoided before reaching T_g, which makes the system heterogeneous.
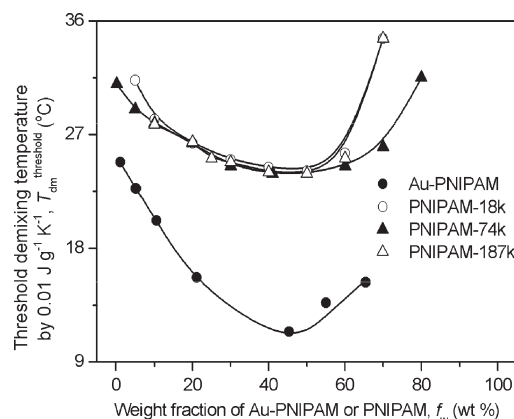

Figure 4. Comparison of the evolution of $T_{dm}^{threshold}$ with f_w for aqueous Au−PNIPAM dispersions and aqueous solutions of PNIPAM of different chain lengths (from ref 11).
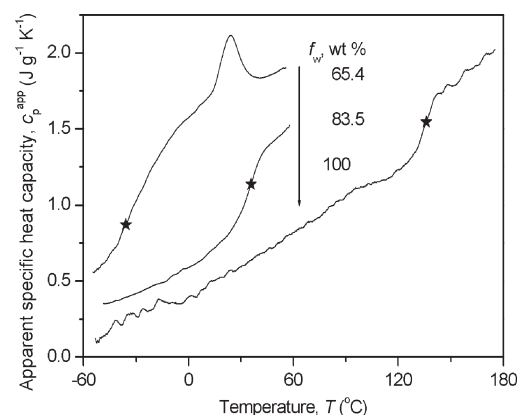

Figure 5. MTDSC c_p^{app} traces during cooling for the detection of T_g in concentrated aqueous Au−PNIPAM dispersions and pure Au−PNIPAM. f_w is indicated. Curves are shifted vertically for clarity.
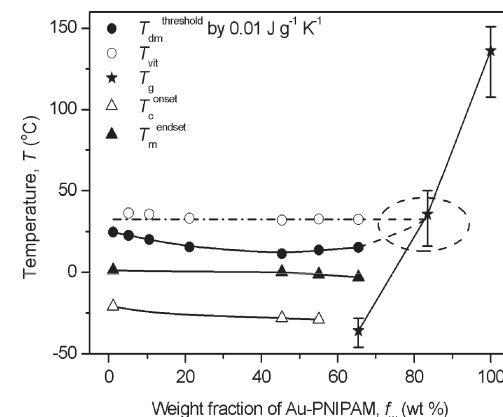

Figure 6. State diagram of aqueous Au−PNIPAM dispersions with $T_{dm}^{threshold}$ by 0.01 J g^{-1} K^{-1}, T_g with a vertical bar indicating the glass transition region, T_c^{onset}, and $T_m^{end\ set}$. The intersection between the $T_{dm}^{threshold}$ line and the T_g line corresponds with T_{vit}, as indicated with the oval.

Figure 6 collects the demixing temperature $T_{dm}^{threshold}$ (from Figure 2), T_g with a vertical bar indicating the whole glass transition region (from Figure 5), the onset temperature of crystallization (T_c^{onset}), and the end-set temperature of melting ($T_m^{end set}$) in a state diagram for aqueous Au−PNIPAM dispersions. Note that the estimated intersection of the demixing temperatures with the glass transition curve corresponds fairly well with T_{vit}, which means partial vitrification occurs in the polymer-rich phase during demixing in zone C[11] and which agrees with the big change in c_p^{app} (Δc_p^{app}) as observed in Figures 1a and 2 for 21.1−65.4 wt %. From the position of T_{vit} with respect to the T_g of the 83.5 wt % dispersion (Figure 2), one can deduce that at T_{vit} a 83.5 wt % polymer-rich phase would be closer to the fully glassy (frozen in) state than to the liquid (mobile) state.

The concept of double subzones introduced for explaining the double demixing peaks observed in very dilute dispersions,[59] with densely packed, less hydrated PNIPAM segments close to the gold surface undergoing the lower temperature transition, and looser, more hydrated PNIPAM segments in the outer layer undergoing the upper temperature transition, is supported by the state diagram (Figure 6). For a given f_w below 45.3 wt %, the local f_w of PNIPAM in the inner layer should be higher than this value, while the local f_w of PNIPAM in the outer layer should be lower than it. Thus, according to the state diagram and Figure 3a, the PNIPAM segments in the inner layer should break the hydrogen bonds, release the water molecules, and collapse at a lower temperature than the segments in the outer layer. With increasing overall f_w, the local f_w of the denser inner layer should increase less significantly than that in the outer one due to the confinement exerted by the gold core. It is worth noting that the estimated volume fraction of PNIPAM segments close to the surface of the gold core amounts to 40−50% (assuming stretched PNIPAM chains extending from the surface and depending on the geometry or surface/volume ratio of the gold core). Thus, for a higher overall f_w, there might be no local f_w difference between the inner and outer layer any more. Consequently, the two phase transitions would merge into one single transition. The double subzones model can also explain the seemingly inconsistent results between the onset of demixing observed in MTDSC ($T_{dm}^{threshold}$) and the cloud point temperature ($T_{dm}^{cloud\ point}$) at f_w of 57 wt % and less (Figure 3a). Indeed, when the inner layer collapses, the outer layer is still hydrophilic. Hence, there should be no (strongly) increased tendency for aggregation of particles, resulting in the absence of a decrease in light transmittance near $T_{dm}^{threshold}$. Only when the outer layer starts collapsing, the outside of the particles becomes hydrophobic and the tendency for aggregation of particles increases, resulting in larger domains and the observed decrease in light transmittance. Moreover, for f_w close to 60 wt %, the PNIPAM layer collapses as a single layer, resulting immediately in the aggregation of larger domains, which explains why in this case the cloud point ($T_{dm}^{cloud\ point}$) is observed closely to the start of the demixing in c_p^{app} ($T_{dm}^{threshold}$). It might indicate that the cloud point is more indicative for $T_{dm}^{threshold}$ of the upper temperature demixing peak. This threshold value cannot be determined accurately in all conditions due to an incomplete separation of both demixing peaks. However, it should be around $T_{dm,lower}^{peak}$, explaining why the cloud point is found near $T_{dm,lower}^{peak}$ for f_w between 1 and 20 wt %. It should be noted that for all dispersions in this work, even for 1.1 wt %, the Au−PNIPAM nanoparticles most likely are aggregated on the mesoscale, which is actually negligible for very dilute dispersions only.[59,63,67]

Having constructed the state diagram and confirmed the plausibility of the double subzones model, the remainder of this paper will focus on the kinetics of the demixing and remixing processes.

Transformation Kinetics. For the two subzones with different local concentration of PNIPAM the transformation kinetics could be expected to be different. Hence, the kinetics of the demixing and remixing events was studied in detail by quasi-isothermal evolutions and through the influence of various modulation frequency and heating and cooling rates. The results will be discussed in relation to previous observations for aqueous PNIPAM[11] solutions and solutions of PNIPAM grafted with poly(oxyethylene) (PEO), PNIPAM-g-PEO.[18] Quasi-isothermal demixing and remixing studies are of particular interest, as the c_p^{app} evolution during these quasi-isothermal experiments can be attributed to morphological developments in the solutions,[11,14,26] with a decreasing c_p^{app} indicating the exchange of a decreasing amount of material through the interface between the coexisting polymer-rich and water-rich phases in the reversible demixing/remixing process, as a result of a decreasing interfacial contact area or a decreasing interdiffusion rate (and vice versa). These quasi-isothermal evolutions of c_p^{app} have been observed in aqueous polymer solutions,[11,26,35,38] hydrogels,[14,26] and polymer blends.[55,68]

Figure 7a shows an overlay of the results for the quasi-isothermal demixing and remixing on the nonisothermal demixing (heating) and subsequent remixing (cooling) for aqueous Au−PNIPAM dispersions with f_w of 21.1 wt %. Figure 7b shows the same results but zooms in on the temperature region corresponding to zone B. Figure 7c displays the corresponding time dependence of c_p^{app} during the quasi-isothermal demixing and remixing at five temperatures. Note that the start points of the quasi-isothermal demixing and remixing are always on the nonisothermal demixing and remixing curves, respectively (Figure 7a). This is due to the fact that all start points are reached by the same temperature program as for the nonisothermal measurements. In nearly all cases, c_p^{app} levels off within 60 min. In experiments with quasi-isothermal segments of up to 1800 min at several temperatures in the phase transition region no further evolution of c_p^{app} was seen after 180 min.

Close to $T_{dm,lower}^{peak}$ (26.0 °C), the largest quasi-isothermal evolutions in c_p^{app} are noted (Figure 7c). The evolution is much faster than for PNIPAM, where it took more than a day to reach the final state.[11]

For the Au−PNIPAM dispersions, the end points of the quasi-isothermal demixing and remixing at a given temperature are always very close to each other and are usually closer to the remixing curve (Figure 7b,c), which indicates that the dispersion evolves to a final state (morphology) at that given temperature, independent of the thermal history.[11,14,26] Remarkably, for temperatures up to 23.0 °C, on the rising side of the demixing peak and well above the demixing temperature of 15.7 °C, the final state curve coincides with the heating curve (Figure 7c). Additionally, at 55.0 °C (zone C), no evolution of c_p^{app} is observed. For aqueous PNIPAM solutions, c_p^{app} becomes time-dependent at temperatures just above the demixing temperature,[11] resulting in time independence in zone A only and time dependence in zones B and C. In contrast, for aqueous Au−PNIPAM dispersions time independence is observed over the first 7 K of zone B and for temperatures in zone C. As a matter of fact, the results tend toward the results for aqueous PNIPAM-g-PEO solutions, where a time-independent response was found over the full temperature interval.[18] The fast response of the latter system was attributed to the presence of the PEO
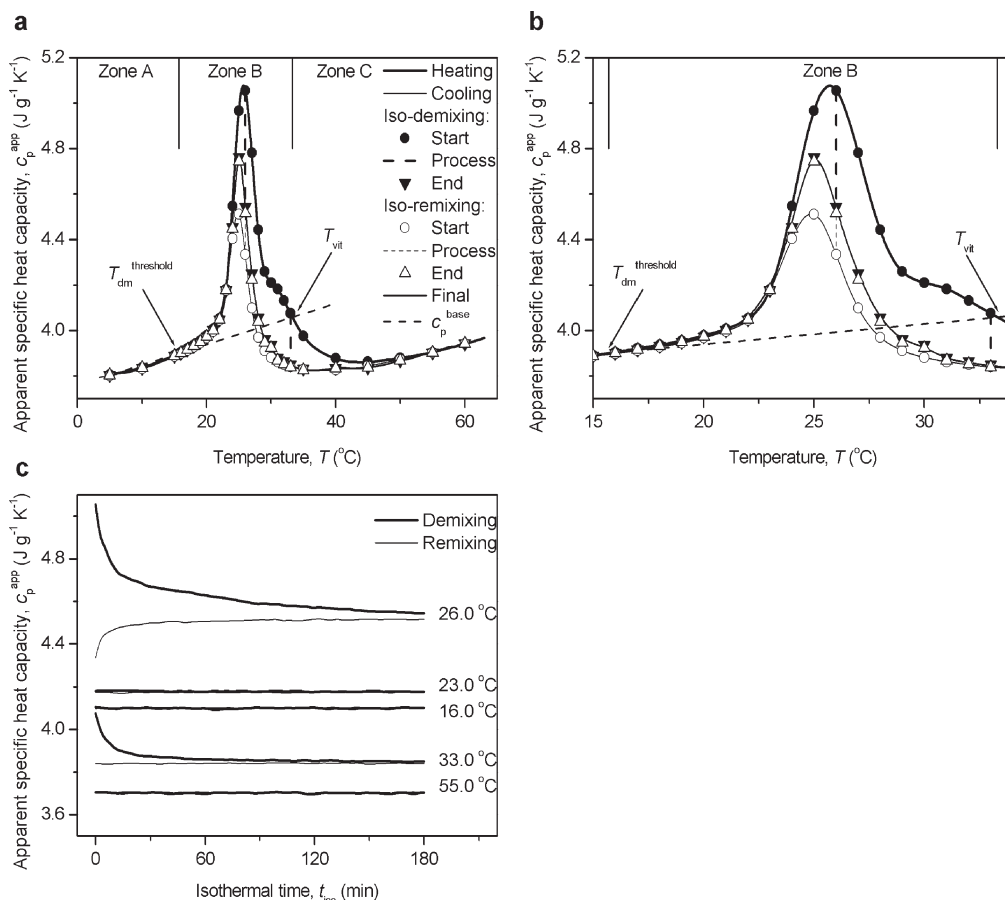
Figure 7. Overlay of the MTDSC c_p^{app} during quasi-isothermal demixing and remixing with nonisothermal demixing (heating) and subsequent remixing (cooling) (a, b) and the time dependence of c_p^{app} during quasi-isothermal demixing (thick curves) and remixing (thin curves) (c) in aqueous Au−PNIPAM dispersions with f_w of 21.1 wt %. The start point of quasi-isothermal demixing is reached by heating at 1.0 K min^{-1} from the homogeneous state at 2.0 °C, where dispersions have been kept isothermally for 30 min. The start point of the quasi-isothermal remixing is reached by cooling at 1.0 K min^{-1} from the heterogeneous state at 65.0 °C, where dispersions have been kept isothermally for 5 min. The quasi-isothermal demixing and remixing processes and their start and end values obtained from (c) are shown in (a) and (b) as vertical dashed lines and symbols, respectively. The final state trace in (a) and (b) is the average of the end values for the quasi-isothermal demixing and remixing at the same temperature (performed over the same temperature range as the nonisothermal measurements using an interval of 1.0 K). In (c), the isothermal demixing and remixing curves at 16.0 and 55.0 °C were shifted by +0.2 and −0.2 J g^{-1} K^{-1}, respectively.

grafts inside the PNIPAM domains, ensuring a fast transport of water even through a partially vitrified matrix.

Figure 8 shows results for the quasi-isothermal demixing and remixing for aqueous Au−PNIPAM dispersions with f_w of 45.3 wt %. The results are quite similar to those for the 21.1 wt % dispersion. Again, the final state curve (nearly) coincides with the heating curve on the rising side of the demixing peak and at temperatures well above the demixing temperature of 11.4 °C (Figure 8c). However, the most important difference is that, as a result of slower remixing, the c_p^{app} curve measured in cooling is below the heating curve, and a quasi-isothermal increase in c_p^{app} toward the final value (on the heating curve) is noted.

Figure 9 shows results for the quasi-isothermal demixing and remixing for aqueous Au−PNIPAM dispersions with f_w of 65.4 wt %. At this concentration, the final state curve (nearly) coincides with the heating and the cooling curve over the full temperature region (Figure 9a,b). Only small changes in c_p^{app} during isothermal demixing or remixing are noted. This indicates that the system is responding quickly enough to the temperature changes to attain its final state (structure) at each temperature while heating or cooling at 1.0 K min^{-1}.

In addition to quasi-isothermal studies, changing the modulation frequency can help elucidate the kinetics of the phase transition, as demixing and remixing processes

will only contribute to c_p^{app} if they are reversible on the time scale of the modulation[11,14,15,26,35,37,38] or if its rate is instantaneously responding to the temperature modulation cycle. Figure 10a shows MTDSC c_p^{app} traces for the non-isothermal demixing (heating) and subsequent remixing (cooling) with various modulation periods p in aqueous dispersions of Au−PNIPAM with f_w of 21.1 wt %. With increasing p, the intensity of the demixing and remixing peaks increases gradually, indicating that a higher fraction of the material can follow the slower modulation and resulting in a decrease of the contribution of the nonreversing heat flow. For the results of Figure 10a, ΔH_{rm}^{nonrev} is about 1.7 J g^{-1} for p of 15 s, about 1.2 J g^{-1} for p of 30 s, about 0.5 J g^{-1} for p of 60 s, and about 0.2 J g^{-1} for p of 120 s. Compared with the demixing, which is a fast process that can almost completely follow the applied modulation even at the lowest p of 15 s used in our experiments, the remixing must be a (considerably) slower process as it can only partially follow the applied modulation. It also explains why the remixing peak is starting earlier (at higher temperature) in HF_{tot} (and HF_{nonrev}) than in HF_{rev} (see Figure 1b). These findings are also supported by experiments at different scan rates. For heating rates between 0.1 and 2.5 K min^{-1}, the same (time-independent) c_p^{app} level is found at 60 °C, indicating a similar (stable) degree of vitrification. However, cooling at 2.5 K min^{-1} results in a
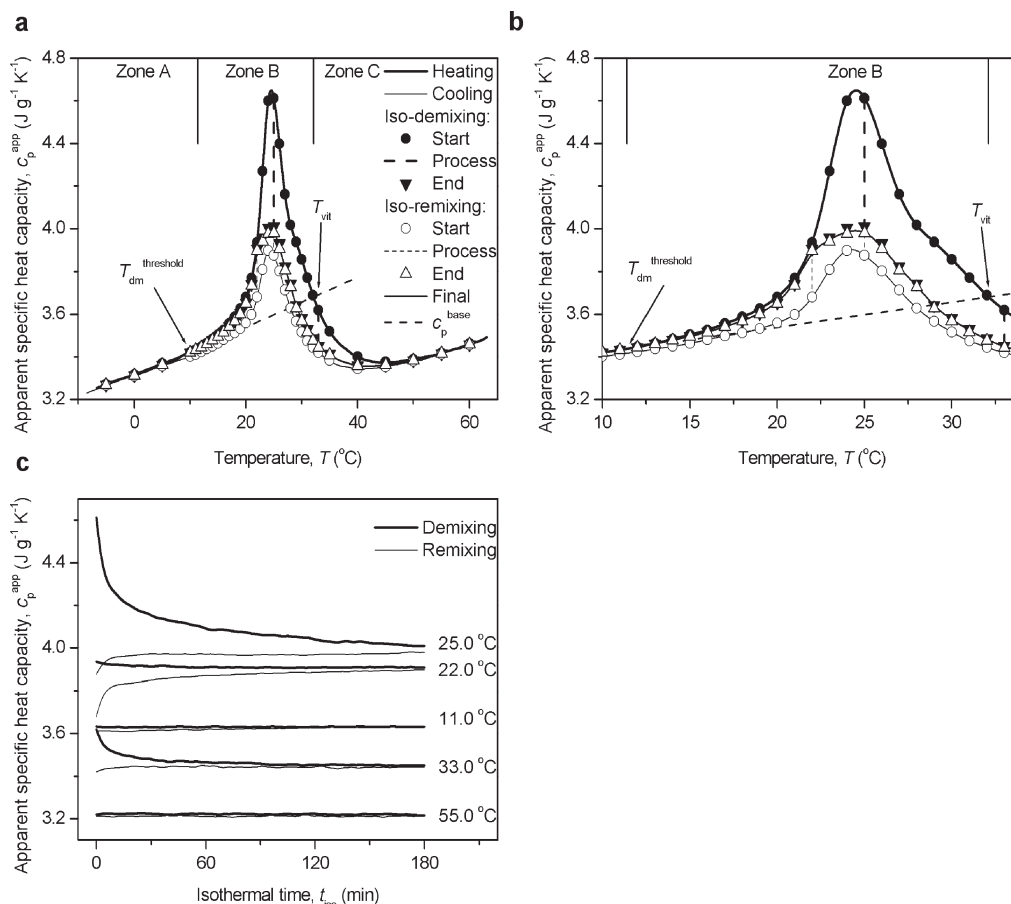
Figure 8. Overlay of the MTDSC c_p^{app} during quasi-isothermal demixing and remixing with nonisothermal demixing (heating) and subsequent remixing (cooling) (a, b) and the time dependence of c_p^{app} during quasi-isothermal demixing (thick curves) and remixing (thin curves) (c) in aqueous Au−PNIPAM dispersions with f_w of 45.3 wt %. See also Figure 7. In (c), the isothermal demixing and remixing curves at 11.0 and 55.0 °C were shifted by +0.2 and −0.2 J g^{-1} K^{-1}, respectively.

lower c_p^{app} in the homogeneous zone A, indicating that (a fraction of) the polymer-rich phase is still partially vitrified. Staying isothermal for a few minutes restores c_p^{app} at its original level, confirming remixing is complete. In addition to the effect of the cooling rate on the remixing, also the evolution of the demixing with heating rate is of interest: the height of the upper temperature demixing peak decreases significantly at a rate of 0.1 K min^{-1}. This can be attributed to a gradual morphological evolution during this slow heating and is in agreement with the decreasing c_p^{app} during quasi-isothermal demixing (see Figure 7).

For aqueous PNIPAM solutions, vitrification is known to have a major effect on the remixing kinetics.[11] Heating PNIPAM solutions long enough above T_{vit} (zone C), either by waiting at higher temperatures or by scanning slowly, results in a gradually increasing degree of vitrification. In the cooling, this results in a decreasing amount of remixing, as deduced from decreasing heats of remixing and (subsequent) demixing and from a lower c_p^{app} at temperatures below and above the phase transition (as the polymer-rich phase remains largely in the fully glassy state). In the aqueous Au−PNIPAM dispersions, vitrification seems to slow down the remixing to a much less extent than for PNIPAM. Nevertheless, from the intersection of the demixing curve with the T_g−composition relation (Figure 6), one can deduce that the polymer-rich phase has to be in a vitrified state at the start of the cooling, and as long as the material is vitrified, one could expect that the interdiffusion and remixing should be fairly slow.

The effect of vitrification was further studied through a long quasi-isothermal stay above T_{vit} and through repeated heating−cooling cycles. Figure 11a shows that c_p^{app} measured in a cooling at 10.0 °C (below the LCST) after stay at 55.0 °C for 5000 min results in a somewhat lower c_p^{app} in the homogeneous zone A, indicating that (a fraction of) the polymer-rich phase is still (partially) vitrified. The remixing enthalpy ΔH_{rm}^{tot} is also about 25% lower. Figure 11b,c illustrates the effect of repeated cycles, showing selected c_p^{app} traces during 45 consecutive heating−cooling cycles of aqueous Au−PNIPAM dispersion with f_w of 21.1 wt %. Although the observed evolutions can be attributed to vitrification, the c_p^{app} level in the homogeneous zone A and the shape of the demixing and remixing peaks are much less markedly influenced than for a comparable experiment with a 50.0 wt % aqueous PNIPAM-25K solution (Figure 11d). In the latter, vitrification of the polymer-rich phase during heating leads to a marked slowdown of the subsequent remixing, resulting in a decrease of the amount of PNIPAM participating in the next cycle and a rapid loss of the thermoresponsivity. As the Δc_p^{app} resulting from demixing is similar for a 21.1 wt % Au−PNIPAM dispersion as for a 20 wt % PNIPAM solution (see Figure 1 and ref 11), a similar degree of vitrification is thought to be reached during heating. Nevertheless, the remixing of the Au−PNIPAM systems is much faster than for PNIPAM. This can probably be attributed to a larger interfacial contact area between the coexistent phases (smaller phases) or to a faster interdiffusion. As in both cases water needs to diffuse into vitrified PNIPAM,
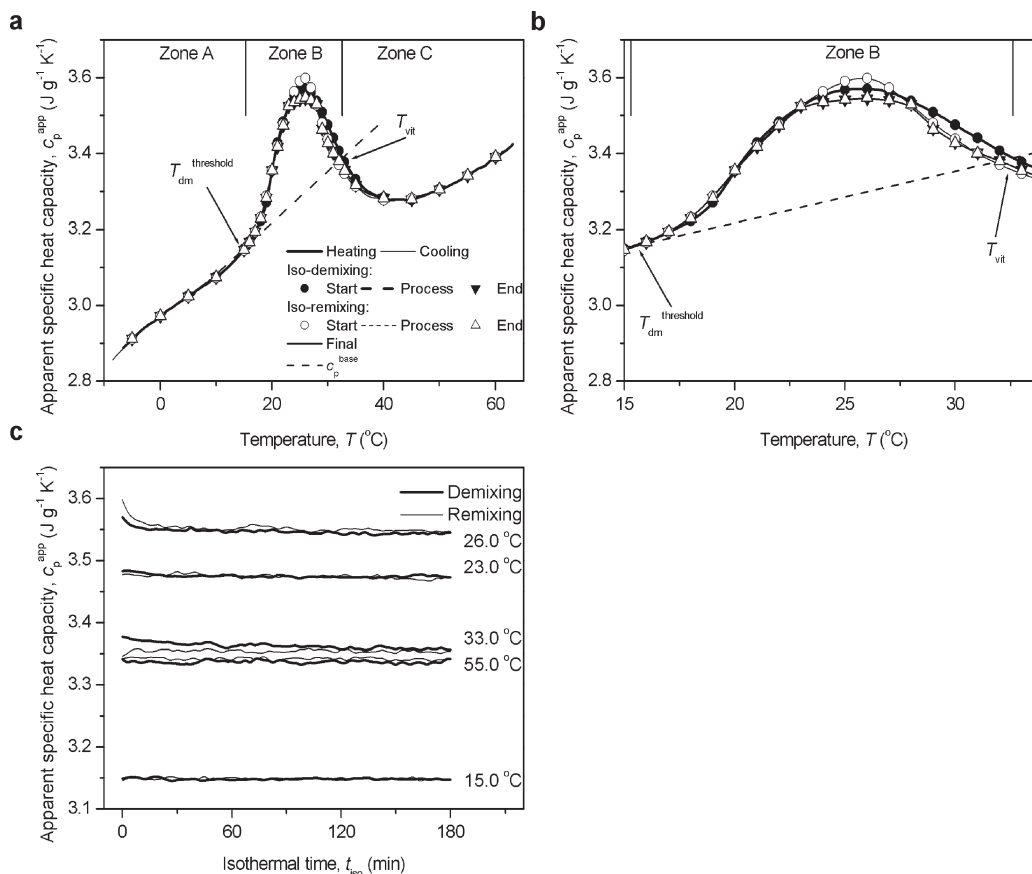
Figure 9. Overlay of the MTDSC c_p^{app} during quasi-isothermal demixing and remixing with nonisothermal demixing (heating) and subsequent remixing (cooling) (a, b) and the time dependence of c_p^{app} during quasi-isothermal demixing (thick curves) and remixing (thin curves) (c) in aqueous Au−PNIPAM dispersions with f_w of 65.4 wt %. See also Figure 7.
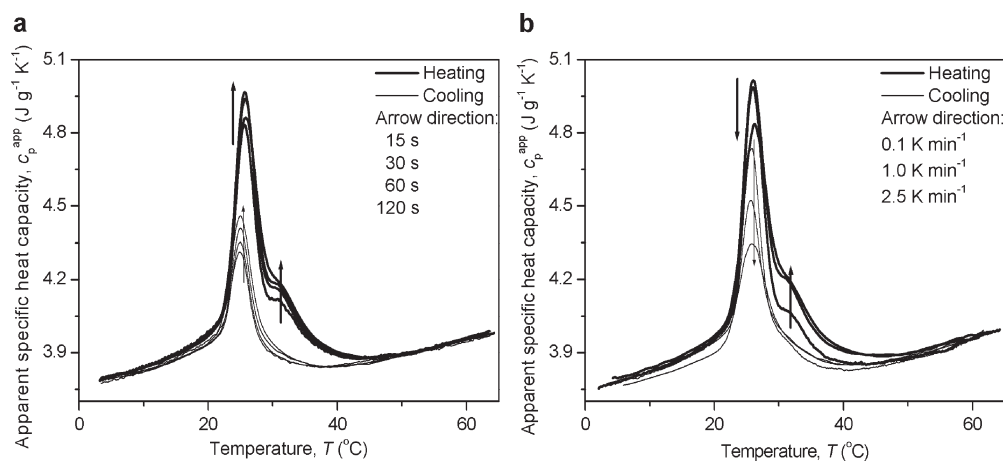

Figure 10. MTDSC c_p^{app} traces during nonisothermal demixing (heating, thick curves) and subsequent remixing (cooling, thin curves) in aqueous Au−PNIPAM dispersions with f_w of 21.1 wt % measured for various modulation periods p (a) and scan rates (b). In (a) the heating and cooling curves with a p of 60 s are fixed. The other three heating curves are, together with their respective cooling curves, shifted vertically and rotated to make all four heating curves coincide at the temperatures of 10.0 and 55.0 °C, respectively.

a smaller diffusion distance might be at the origin of the much faster response of the Au−PNIPAM dispersions. Similarly, by incorporating PEO grafts inside the PNIPAM domains, a fast transport of water through a partially vitrified matrix could be ensured, leading to a faster thermoresponsive behavior.[18] For the Au−PNIPAM dispersions, water might remain within the particles, close to the core where the PNIPAM chains might not be able to fully collapse and remain in a more stretched state as a result of

steric hindrance between neighboring anchored chains. The water stored close to the Au core might be the main reason for a fast (partial) devitrification and the faster response of the Au−PNIPAM dispersions (as compared to pure PNIPAM). For the highest concentrations, water remaining between the (entangled) collapsed Au−PNIPAM nanoparticles might result in the nearly reversible behavior observed for f_w of 65.4 wt %. For less concentrated dispersions, the water expelled during the collapse of the (less entangled)
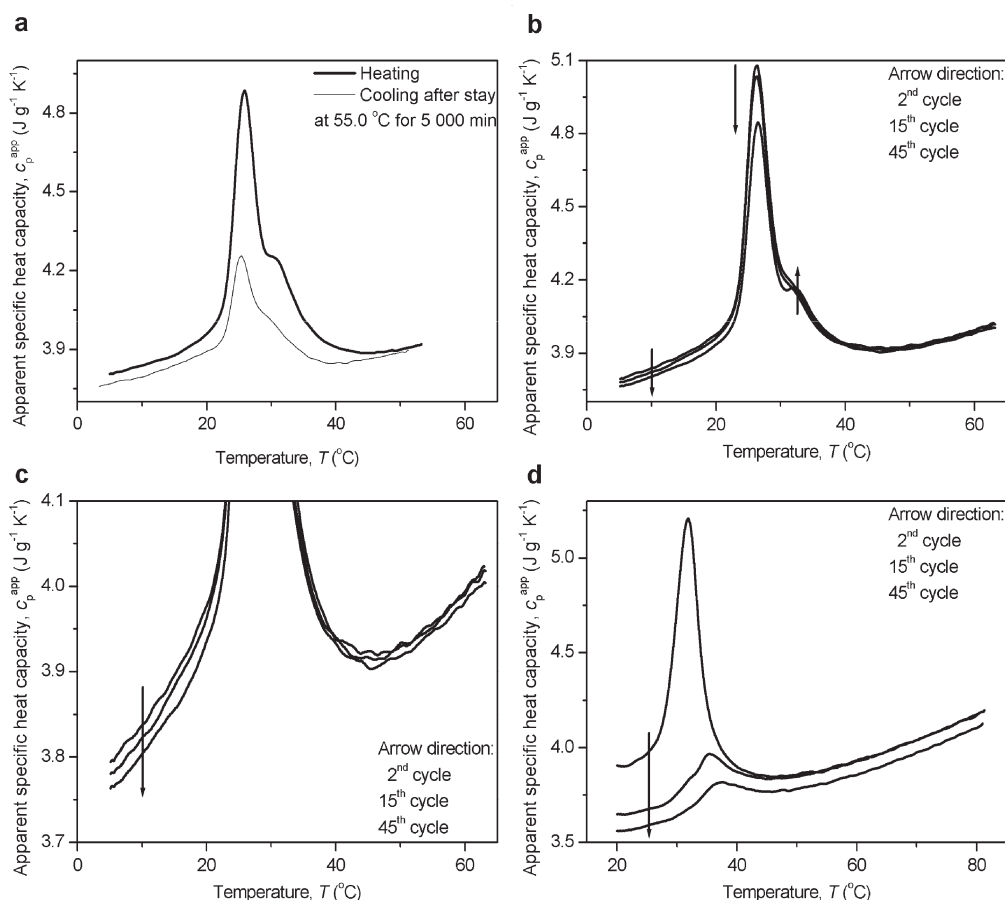
a

b

c

d

Figure 11. Effect of vitrification in MTDSC c_p^{app} traces during nonisothermal demixing (heating, thick curves) and subsequent remixing (cooling, thin curves) in aqueous dispersions of Au−PNIPAM with f_w of 21.1 wt % (a−c) and aqueous solutions of PNIPAM-25K with f_w of 50.0 wt % (d). (a) Remixing after a quasi-isothermal stay at 55.0 °C for 5000 min. (b−d) Selected heating segments of an experiment of 45 consecutive heating−cooling cycles.

particles might form larger phase domains, resulting in the need for diffusion through the (partially) vitrified PNIPAM over longer distances and a remixing that is somewhat slower than for the lowest and highest concentrations but still markedly faster than for pure PNIPAM.

Conclusions

The demixing and remixing kinetics in aqueous dispersions of Au−PNIPAM were studied by means of MTDSC in both nonisothermal and quasi-isothermal modes. The dispersions follow an LCST phase behavior with a minimum at about 11.4 °C for f_w of 45.3 wt % (based on the threshold temperature). Comparison with the aqueous solutions of PNIPAM with different molar masses shows that attaching the chains to the gold core reduces the miscibility of PNIPAM with water. The nonisothermal measurements show double demixing peaks in both the *HF* and c_p^{app} traces for dispersions with f_w below 50 wt %, with a lower temperature phase transition corresponding to a denser inner layer of PNIPAM segments near the surface of the gold core and an upper temperature transition corresponding to a less dense outer layer. Overall, the response for Au−PNIPAM dispersions is faster than for PNIPAM, which might be the result of water remaining finely dispersed within the polymer matrix. Water might remain present close to the gold nanoparticles due to restrictions on the collapse of the PNIPAM chains as a result of steric hindrance by neighboring anchored chains. We expect that similar effects might also be occurring in aqueous dispersions of core−shell particles with a solid polymer core and a water-soluble shell.

References and Notes

(1) Schild, H. G. *Prog. Polym. Sci.* **1992**, *17*, 163–249.
(2) Tiktopulo, E. I.; Bychkova, V. E.; Ricka, J.; Ptitsyn, O. B. *Macromolecules* **1994**, *27*, 2879–2882.
(3) Tiktopulo, E. I.; Uversky, V. N.; Lushchik, V. B.; Klenin, S. I.; Bychkova, V. E.; Ptitsyn, O. B. *Macromolecules* **1995**, *28*, 7519–7524.
(4) Wang, X.; Qiu, X.; Wu, C. *Macromolecules* **1998**, *31*, 2972–2976.
(5) Lowe, T. L.; Tenhu, H.; Tylli, H. *J. Appl. Polym. Sci.* **1999**, *73*, 1031–1039.
(6) Kujawa, P.; Winnik, F. M. *Macromolecules* **2001**, *34*, 4130–4135.
(7) Avoce, D.; Liu, H. Y.; Zhu, X. X. *Polymer* **2003**, *44*, 1081–1087.
(8) Balamurugan, S.; Mendez, S.; Balamurugan, S. S.; O'Brien, M. J. II; Lopez, G. P. *Langmuir* **2003**, *19*, 2545–2549.
(9) Nichifor, M.; Zhu, X. X. *Polymer* **2003**, *44*, 3053–3060.
(10) Stieger, M.; Richtering, W. *Macromolecules* **2003**, *36*, 8811–8818.
(11) Van Durme, K.; Van Assche, G.; Van Mele, B. *Macromolecules* **2004**, *37*, 9596–9605.
(12) Okada, Y.; Tanaka, F. *Macromolecules* **2005**, *38*, 4465–4471.
(13) Kita, R.; Wiegand, S. *Macromolecules* **2005**, *38*, 4554–4556.
(14) Van Durme, K.; Van Mele, B.; Loos, W.; Du Prez, F. E. *Polymer* **2005**, *46*, 9851–9862.
(15) Van Durme, K.; Rahier, H.; Van Mele, B. *Macromolecules* **2005**, *38*, 10155–10163.
(16) Kujawa, P.; Segui, F.; Shaban, S.; Diab, C.; Okada, Y.; Tanaka, F.; Winnik, F. M. *Macromolecules* **2006**, *39*, 341–348.
(17) Kujawa, P.; Tanaka, F.; Winnik, F. M. *Macromolecules* **2006**, *39*, 3048–3055.
(18) Van Durme, K.; Van Assche, G.; Aseyev, V.; Raula, J.; Tenhu, H.; Van Mele, B. *Macromolecules* **2007**, *40*, 3765–3772.

(19) Uyama, H.; Kobayashi, S. *Chem. Lett.* **1992**, 1643–1646.
(20) Diab, C.; Akiyama, Y.; Kataoka, K.; Winnik, F. M. *Macromolecules* **2004**, *37*, 2556–2562.
(21) Park, J.-S.; Akiyama, Y.; Winnik, F. M.; Kataoka, K. *Macromolecules* **2004**, *37*, 6786–6792.
(22) Park, J.-S.; Kataoka, K. *Macromolecules* **2007**, *40*, 3599–3609.
(23) Demirel, A. L.; Meyer, M.; Schlaad, H. *Angew. Chem., Int. Ed.* **2007**, *46*, 8622–8624.
(24) Laukkanen, A.; Hietala, S.; Maunu, S. L.; Tenhu, H. *Macromolecules* **2000**, *33*, 8703–8708.
(25) Maeda, Y.; Nakamura, T.; Ikeda, I. *Macromolecules* **2002**, *35*, 217–222.
(26) Van Durme, K.; Verbrugghe, S.; Du Prez, F. E.; Van Mele, B. *Macromolecules* **2004**, *37*, 1054–1061.
(27) Laukkanen, A.; Valtola, L.; Winnik, F. M.; Tenhu, H. *Macromolecules* **2004**, *37*, 2268–2274.
(28) Okhapkin, I. M.; Bronstein, L. M.; Makhaeva, E. E.; Matveeva, V. G.; Sulman, E. M.; Sulman, M. G.; Khokhlov, A. R. *Macromolecules* **2004**, *37*, 7879–7883.
(29) Laukkanen, A.; Winnik, F. M.; Tenhu, H. *Macromolecules* **2005**, *38*, 2439–2448.
(30) Kharlampieva, E.; Pristinski, D.; Sukhishvili, S. A. *Macromolecules* **2007**, *40*, 6967–6972.
(31) Gundlach, D. P.; Burdett, K. A. *J. Appl. Polym. Sci.* **1994**, *51*, 731–737.
(32) Schaefer-Soenen, H.; Moerkerke, R.; Berghmans, H.; Koningsveld, R.; Dusek, K.; Solc, K. *Macromolecules* **1997**, *30*, 410–416.
(33) Moerkerke, R.; Meeussen, F.; Koningsveld, R.; Berghmans, H.; Mondelaers, W.; Schacht, E.; Dusek, K.; Solc, K. *Macromolecules* **1998**, *31*, 2223–2229.
(34) Meeussen, F.; Bauwens, Y.; Moerkerke, R.; Nies, E.; Berghmans, H. *Polymer* **2000**, *41*, 3737–3743.
(35) Swier, S.; Van Durme, K.; Van Mele, B. *J. Polym. Sci., Part B: Polym. Phys.* **2003**, *41*, 1824–1836.
(36) Nies, E.; Ramzi, A.; Berghmans, H.; Li, T.; Heenan, R. K.; King, S. M. *Macromolecules* **2005**, *38*, 915–924.
(37) Van Durme, K.; Van Mele, B.; Bernaerts, K. V.; Verdonck, B.; Du Prez, F. E. *J. Polym. Sci., Part B: Polym. Phys.* **2006**, *44*, 461–469.
(38) Van Durme, K.; Van Assche, G.; Nies, E.; Van Mele, B. *J. Phys. Chem. B* **2007**, *111*, 1288–1295.
(39) Solc, K.; Dusek, K.; Koningsveld, R.; Berghmans, H. *Collect. Czech. Chem. Commun.* **1995**, *60*, 1661–1688.
(40) Afroze, F.; Nies, E.; Berghmans, H. *J. Mol. Struct.* **2000**, *554*, 55–68.
(41) Reading, M. *Trends Polym. Sci.* **1993**, *8*, 248–253.
(42) Wunderlich, B.; Jin, Y.; Boller, A. *Thermochim. Acta* **1994**, *238*, 277–293.
(43) Reading, M.; Luget, A.; Wilson, R. *Thermochim. Acta* **1994**, *238*, 295–307.
(44) *Modulated-Temperature Differential Scanning Calorimetry: Theoretical and Practical Applications in Polymer Characterization (Hot Topics in Thermal Analysis and Calorimetry)*; Reading, M., Hourston, D. J., Eds.; Springer: London, UK, 2006.
(45) Van Assche, G.; Van Hemelrijck, A.; Rahier, H.; Van Mele, B. *Thermochim. Acta* **1995**, *268*, 121–142.
(46) Swier, S.; Van Mele, B. *J. Polym. Sci., Part B: Polym. Phys.* **2003**, *41*, 594–608.
(47) Swier, S.; Van Mele, B. *Macromolecules* **2003**, *36*, 4424–4435.
(48) Ishikiriyama, K.; Wunderlich, B. *J. Polym. Sci., Part B: Polym. Phys.* **1997**, *35*, 1877–1886.
(49) Minakov, A. A.; Schick, C. *Thermochim. Acta* **1999**, *330*, 109–119.
(50) Miltner, H. E.; Rahier, H.; Pozsgay, A.; Pukanszky, B.; Van Mele, B. *Compos. Interfaces* **2005**, *12*, 787–803.
(51) Miltner, H. E.; Van Assche, G.; Pozsgay, A.; Pukanszky, B.; Van Mele, B. *Polymer* **2006**, *47*, 826–835.
(52) Zhao, J.; Swinnen, A.; Van Assche, G.; Manca, J.; Vanderzande, D.; Van Mele, B. *J. Phys. Chem. B* **2009**, *113*, 1587–1591.
(53) Dreezen, G.; Groeninckx, G.; Swier, S.; Van Mele, B. *Polymer* **2001**, *42*, 1449–1459.
(54) Swier, S.; Pieters, R.; Van Mele, B. *Polymer* **2002**, *43*, 3611–3620.
(55) Pieters, R.; Miltner, H. E.; Van Assche, G.; Van Mele, B. *Macromol. Symp.* **2006**, *233*, 36–41.
(56) Swier, S.; Van Mele, B. *Polymer* **2003**, *44*, 2689–2699.
(57) Binkert, Th.; Oberreich, J.; Meewes, M.; Nyffenegger, R.; Ricka, J. *Macromolecules* **1991**, *24*, 5806–5810.
(58) Zhu, P. W.; Napper, D. H. *J. Colloid Interface Sci.* **1994**, *164*, 489–494.
(59) Shan, J.; Chen, J.; Nuopponen, M.; Tenhu, H. *Langmuir* **2004**, *20*, 4671–4676.
(60) Shan, J.; Zhao, Y.; Granqvist, N.; Tenhu, H. *Macromolecules* **2009**, *42*, 2696–2701.
(61) Xu, J.; Luo, S.; Shi, W.; Liu, S. *Langmuir* **2006**, *22*, 989–997.
(62) Luo, S.; Xu, J.; Zhu, Z.; Wu, C.; Liu, S. *J. Phys. Chem. B* **2006**, *110*, 9132–9139.
(63) Shan, J.; Nuopponen, M.; Jiang, H.; Kauppinen, E.; Tenhu, H. *Macromolecules* **2003**, *36*, 4526–4533.
(64) Schild, H. G.; Tirrell, D. A. *J. Phys. Chem.* **1990**, *94*, 4352–4356.
(65) Van Durme, K.; Delellio, L.; Kudryashov, E.; Buckin, V.; Van Mele, B. *J. Polym. Sci., Part B: Polym. Phys.* **2005**, *43*, 1283–1295.
(66) Israelachvili, J. N. *Intermolecular and Surface Forces*; Academic Press: London, 1992.
(67) Raula, J.; Shan, J.; Nuopponen, M.; Niskanen, A.; Jiang, H.; Kauppinen, E. I.; Tenhu, H. *Langmuir* **2003**, *19*, 3499–3504.
(68) Pieters, R. Kinetics of Phase Transformations in Polymer Blends by Means of Modulated Temperature DSC. Ph.D. Thesis, Vrije Universiteit Brussel, Brussels, Belgium, **2005**.